Use of Ultra-Small-Angle X-ray Scattering To Measure Grain Size of Lamellar Styrene−Butadiene Block Copolymers

Randall T. Myers and Robert E. Cohen*

Department of Chemical Engineering, Massachusetts Institute of Technology, Cambridge, Massachusetts 02139

Anuj Bellare

Department of Orthopedic Surgery, Brigham and Women's Hospital, Harvard Medical School, Boston, Massachusetts 02115

Received October 23, 1998; Revised Manuscript Received January 22, 1999

ABSTRACT: Simultaneous determination of the lamellar morphological length scale and the grain size of several low molecular weight heterogeneous styrene−butadiene block copolymers was accomplished through the use of ultra-small-angle X-ray scattering measurements. NIST's X23A3 Ultra SAXS beamline of the National Synchotron Light Source in the Brookhaven National Laboratory provided a scattering vector, q, from 0.0004 to 0.1 Å^{-1}. Many of the block copolymer specimens display a clearly resolvable peak in the Ultra SAXS region, and grain size was determined using the spherical form factor. Determination of Porod's law constant and the value of the scattering invariant provided a preliminary verification of the proposed scattering mechanism by solving for the contrast factor and the volume fraction of the grain boundaries in these specimens. Grain size in a given polymer was a function of annealing temperature and time. For the case of a block copolymer swollen with varying amounts of cumene, both the lamellar repeat distance, d, and the grain size, D, increased with the cube root of the volume fraction of solvent over the concentration range examined.

Introduction

It is known that appropriate processing techniques can produce essentially perfectly ordered block copolymer morphologies with a single texture extending throughout the macroscopic dimensions of a specimen.[1] The characteristic repeating length scale, d, of these morphologies is dictated by the molecular weights of the constituent block sequences and is on the order of 100 Å. In the absence of extraordinary processing procedures, a second important length scale appears in the block copolymer. The perfection of the morphology is broken up into grains, each of which contains the ordered morphology of length scale d but with essentially random orientation relative to the specimen boundaries. The kinetics of grain growth in block copolymers has been examined extensively by Balsara et al.[2−6] These grains typically exhibit a characteristic size, D, which is one or more orders of magnitude larger than the morphological length scale, d.

The grainy structure can influence physical properties. For example, gas transport in a grainy lamellar SB diblock is significantly different from that observed in specimens specially processed for series or parallel permeation.[7,8] It is believed that the size of the grains may affect physical properties, and thus it is important to have a robust technique for grain size measurement. We have attempted to characterize grain size using transmission electron microscopy (TEM). Although we can sucessfully verify the existence of grains and grain boundaries in this way (Figure 1), we have been unable to produce the appropriately uniform, large-area ultramicrotomed sections required to obtain a meaningful measurement of grain size. Ongoing collaborative work that combines TEM and high-resolution SEM shows promise for direct imaging of a statistically significant population of grains.[9]

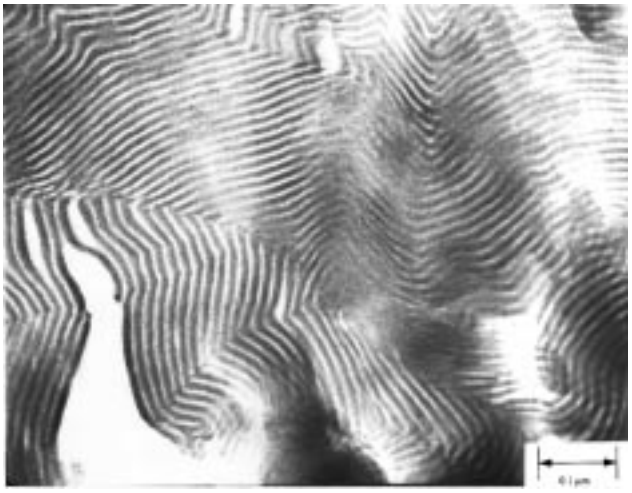

Figure 1. Transmission electron micrograph of the 9900/9700 styrene−1,2-butadiene block copolymer (S12B10) cast from chloroform, ultramicrotomed and stained with OsO_4.

Conventional small-angle X-ray scattering (SAXS) techniques have been employed for decades to characterize block copolymers at the morphological length scale d.[10,11] Recently, Ultra SAXS beamlines have been constructed to probe significantly larger morphological features.[12] The direct and nondestructive examination of grains in bulk, three-dimensional specimens via Ultra SAXS is advantageous in our ongoing effort to connect mechanical behavior with grain structure in block copolymers. It is the purpose of this paper to demonstrate that Ultra SAXS can be used to characterize bulk specimens of block copolymers simultaneously at both the lamellar morphological length scale, d, and the grain length scale, D.

10.1021/ma9816618 CCC: $18.00
Published on Web 03/24/1999

Experimental Section

For the first part of this study, three low-molecular weight styrene−butadiene block copolymers were used: 9400/9000, 14800/14100, and 9900/9700. All were synthesized and sold by Polymer Source, Inc., and have polydispersities ranging from 1.02 to 1.03. The first two contain about 90% 1,4-butadiene in the rubber block, while the third contains 90% 1,2-butadiene in the rubber block. The three polymers will be referred to as SB9, SB15, and S12B10.

The polymers were dissolved in various solvents and static cast. In this paper we report results for specimens cast from solvents of relatively high volatility, namely choloform and methylene chloride (vapor pressures at 25 °C are 26 and 58 kPa, respectively). Annealing at elevated temperatures leads to growth of grains.[2] For the low-molecular weight SB diblock colpolymers examined here, annealing at 75 °C produced measurable increases in grain size over the period of several hours.

To avoid the inevitable criticism that X-ray scattering at very low angles is dominated by the presence of voids in rigid undiluted polymers, a second set of experiments involved swelling a styrene−butadiene block copolymer with solvent. Phillips KR03 Resin, a styrene−butadiene block copolymer, was used for these experiments. It contains 23 wt % butadiene units and has a molecular weight of 217 000 g/mol. More details of the molecular architecture and TEM characterization of the lamellar morphology appear elsewhere.[13,14] These K-resin pellets (ca. 2 mm diameter spheres) were mixed with various amounts of cumene. Polymer volume fractions of 0.66, 0.57, 0.45, and 0.29 were used. The samples were prepared by adding the selected amount of cumene to the KR03 resin in a closed container; the components were allowed to mix with occasional gentle agitation over a period of weeks until a uniform, pourable, transparent material was obtained. Immediately prior to X-ray measurements, the mixtures were loaded into specially prepared specimen cells with Kapton windows. Essentially no solvent evaporation occurred during the processing and X-ray examination of the specimens. On the basis of the methodologies used for specimen preparation, it was anticipated that whatever preexisting grain structure was present in the K-resin pellets would remain intact in the final specimens, albeit swollen by the cumene solvent. For comparative purposes, Ultra SAXS scattering of a pure KR03 pellet was measured.

The Ultra SAXS experiments were performed at the Brookhaven National Laboratory on the X23A3 beamline operated by the National Institute of Standards and Technology. The available range of scattering vector, $q = (4\pi/\lambda) \sin \theta$, was 0.1−0.0004 Å^{-1}, where θ is one-half the scattering angle and $\lambda = 1.299$ Å is the X-ray wavelength.[12] The X-ray source was collimated using two orthogonal pairs of slits to produce a beam with a square cross section of 0.2 mm × 0.2 mm. Both the X-ray beam and the detector (scintillation counter) with a 5 mm × 5 mm window contributed to smearing effects. The scattering data were desmeared to account for the geometry of the X23A3 beamline using software provided by Dr. Gabrielle Long of the National Institute of Standards and Technology and designed for this specific beamline. The program incorporated the methodology of Lake.[15] Although desmearing altered to a small extent the shapes, locations, and magnitudes of the peaks in the scattering curves, there was no case in which desmearing caused a peak to appear when none was present in the smeared data.

Results

Figure 2 is a set of double-logarithmic plots of absolute intensity, I, vs scatering vector, q, for sample S12B10 (9900/9700). Two peaks are observed in the scattering curves. The peak at higher q appears in the conventional SAXS regime and corresponds to the periodic lamellar morphology of the SB diblock copolymer. The lamellar spacing $d = 2\pi/q_{MAX} = 170$ Å is essentially unchanged by the annealing protocol described in the figure. The position of the peak at the left varies with annealing time; the peaks lie in a range of q corresponding to a characteristic dimension of about 1 μm. As discussed in detail below, we assosciate this low-q peak with the presence of grains in the materials. For the present we note that continued annealing shifts the peak to lower values of q, corresponding to a larger material length scale. We also note that all of the data below about $q = 0.01$ were accessible only through the use of the Ultra SAXS beamline. Conventional point collimation 2D SAXS experiments in our own laboratory faithfully reproduce the peak shapes and locations above $q = 0.01$. Also in Figure 2 there is a clearly discernible straight line regime of all the scattering curves to the right of the low-q peak. The log−log slope in this region of the scattering curves is −4. Even though the −4 slope is a very good fit over a significant range of the data, we checked carefully to determine whether there were any systematic trends in the deviation function, $C_1 - iq^4$ where C_1 is the fitted value of the Porod law constant. The calculated deviations were about 2 orders of magnitude smaller than C_1, and no systematic trend was observed in terms of their dependence on q. Significant deviations from the slope of −4 occur near $q = 0.01$ where the high-q peak overlaps the descending data from the low-q peak.

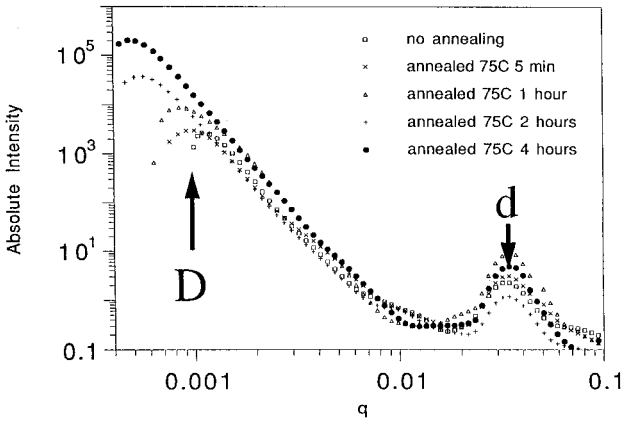

Figure 2. Logarithm of absolute intensity vs log q at various annealing times for the 9900/9700 styrene−1,2-butadiene block copolymer (S12B10) cast from methylene chloride. The right peaks correspond to the interlamellar spacing, d, and the left peaks refer to the grain size, D.

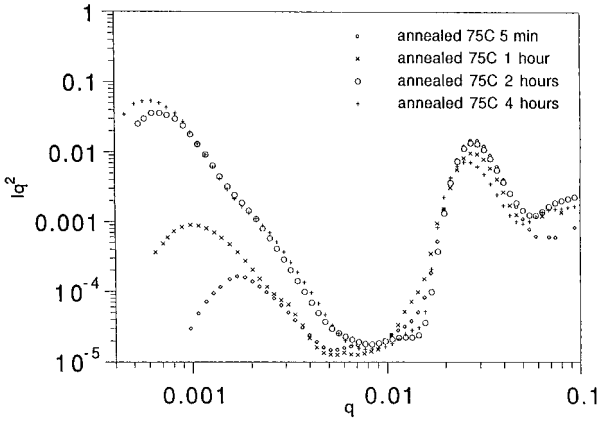

Figure 3. Logarithm of Iq^2 vs log q at various annealing times for the 14800/14100 styrene−1,4-butadiene block copolymer (SB15) cast from chloroform.

Figure 3 presents similar results for the case of sample SB15 (14800/14100). Here the log−log plots are

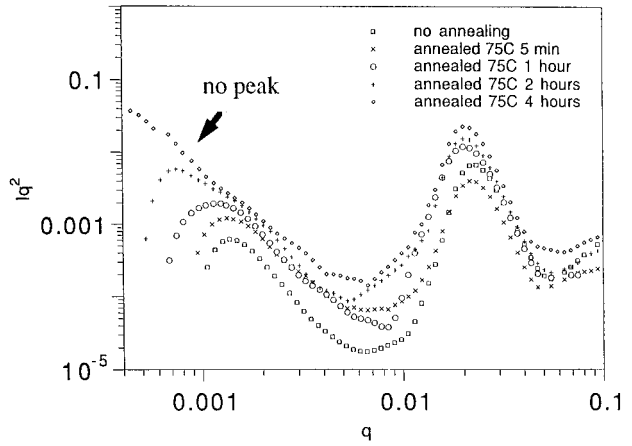

Figure 4. Logarithm of Iq^2 vs log q at various annealing times for the 9400/9000 styrene−1,4-butadiene block copolymer (SB9) cast from chloroform.

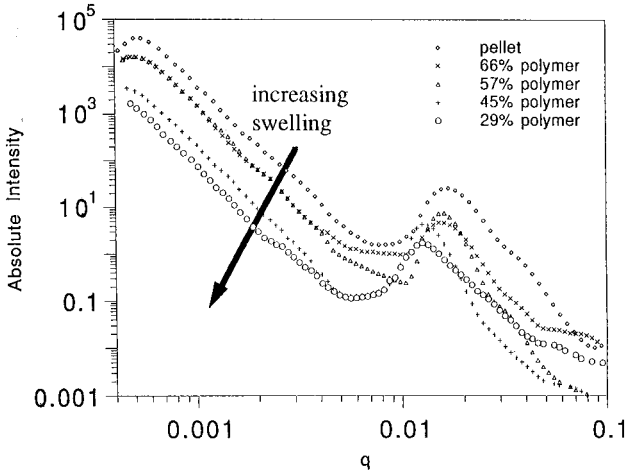

Figure 5. Logarithm of absolute intensity as a function of log q for KR03 resin diluted with various amounts of cumene.

presented in the familiar format of Iq^2 vs q. Again the lamellar spacing (d = 230 Å for this polymer) remains essentially unchanged with time while the low-q peak shifts with annealing by an amount that corresponds to about a factor of 3 in morphological length scale. The data at the lowest values of q in both Figures 2 and 3 fall off in the direction of zero intensity; this trend, coupled with the exceedingly low value of q at the low end of the Ultra SAXS resolution, facilitates calculation of the Ultra SAXS invariant, discussed below, with insignificant low-q truncation error.

Figure 4 is another very similar data set, in this case for sample SB9 (9400/9000). The Iq^2 vs q plots are presented in an expanded scale. The lamellar spacing, d, is centered around a value of 290 Å, and the peak shows a small but noticeable drift toward lower q with annealing. This data set also shows peaks in the Ultra SAXS region of the scattering curves for four of the five specimens. The annealing protocol of 75 °C for 4 h has resulted in a growth of the grain structure to a degree that the length scale is not resolvable as a peak. There is a suggestion that the data points are leveling off at the very lowest q values for this specimen.

Figure 5 presents intensity, I, versus scattering vector, q, results for the cumene swollen samples of the KR03 resin. In this case there is a clear and systematic shift of the lamellar, d, peak to lower values of q as the amount of cumene increases from 0 to 61 vol %. There is a corresponding decrease in the level of scattered X-ray intensity over the entire range of q owing to the reduction of the contrast factor which accompanies the addition of cumene solvent. The unswollen and lightly swollen specimens reveal a peak in the Ultra SAXS region while for the more highly swollen specimens, this peak appears to be shifted to the left, beyond the lower limit of q for the instrument. The q^{-4} dependence of the intensity is preserved in the region of q to the right of the low-q peak for all of the specimens of Figure 5.

Discussion

The results presented above are representative of, but only a minor fraction of, the numerous data sets we have obtained over the course of 18 months and four sessions at the Brookhaven facility. Repeated analysis of individual specimens over this time frame shows excellent repeatablity and reproducibility of all the features of the scattering curves noted above. Thus, the experimental facts are clearly depicted in Figures 2−5. At this point we are faced with a choice. We could assosciate the peak at the left side of each scattering curve with a dimension, $D = 2\pi/q_{max}$, characteristic of the grain structure in the materials; from this simple analysis we would be able to proceed with our structure/property work which aims to correlate grain structure with mechanical behavior, using Ultra SAXS as our robust morphological characterization technique. We are proceeding in this direction at the present time. However, there is a school of thought that expects a mechanistic explanation of the observed scattering phenomenon. We therefore offer in the sections that follow our best current explanation of the mechanism that underlies the low-q peaks seen in the scattering curves shown above. We recognize that other explanations may be offered in the future, and we welcome any debate over mechanism that may arise from the results presented here. The novel and interesting experimental observations presented here and the trends contained therein will of course be unaltered by arguments over mechanisms. Similar analytical techniques to those presented below have recently been employed on scattering data of semicrystalline polymers by Murthy and colleagues as well as by Donald et al.[16−18]

Mechanism of Scattering. There have been studies focused on the detailed structure of grain boundary morphologies in styrene−butadiene block copolymers.[19−23] In these detailed microscopic observations there are clear suggestions that the local composition in the grain boundaries is different from the overall mean composition of the material. It is also known that a free surface leads to an altered local composition in block copolymers,[24] and we make the assumption that similar, although perhaps smaller, compositions fluctuations arise at the grain boundaries. We will test the internal consistency of this assumption later in the analysis, recognizing that the assumed contrast factor, $(\rho_{GB} - \rho_m)^2$, must always lie between zero and either $(\rho_s - \rho_m)^2$ or $(\rho_b - \rho_m)^2$. See Figure 6 for a definition of the various subscripts on the densities, ρ.

In the very low-q range (below about 0.005), the X-rays are oblivious of the short-range lamellar structure of the length scale, d, and are influenced by the mean grain density, ρ_m, over the entire volume of the grain. The presence of a coating or shell of grain boundary material with a local density, $\rho_{GB} \neq \rho_m$, provides a source of scattering contrast in a manner not

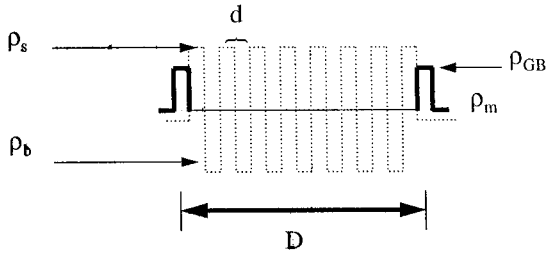

Figure 6. Schematic representation of the proposed mechanism. The dark lines represent the electron density differences represented in the Ultra SAXS region corresponding to the grain size. The electron density differences relating to interlamellar spacing are ghosted in.

Table 1. Values of Grain Size, *D*; Phase Fraction, ϕ; and Electron Density Differences, $(\Delta\rho)^2 = (\rho_{GB} - \rho_m)^2$, as a Function of Annealing Time at 75 °C for 9900/9700 Styrene−1,2-Butadiene (S12B10)

annealing time	D (μm)	$(\Delta\rho)^2$	ϕ	D/d
none	0.67	3.70E−6[a]	0.106	39
5 min	0.74	3.84E−6	0.104	44
1 h	0.80	6.90E−6	0.108	47
2 h	1.28	8.80E−6	0.108	75
4 h	1.40	9.98E−6	0.102	82

[a] Read as 3.70×10^{-6}.

Table 2. Values of Grain Size, *D*; Phase Fraction, ϕ; and Electron Density Differences, $(\Delta\rho)^2 = (\rho_{GB} - \rho_m)^2$ as a Function of Annealing Time at 75 °C for 14800/14100 Styrene−1,4-Butadiene (SB15)

annealing time	D (μm)	$(\Delta\rho)^2$	ϕ	D/d
5 min	0.47	3.75E−7[a]	0.093	20
1 h	0.81	1.27E−6	0.092	35
2 h	1.17	2.33E−5	0.101	51
4 h	1.29	3.27E−5	0.103	56

[a] Read as 3.75×10^{-7}.

unlike the scattering of radiation in foams.[25−27] We proceed with a quantitative analysis of our scattering data along the lines of the mechanism outlined in Figure 6. Instead of employing a quasi-Bragg analysis or a correlation function[28] approach to calculate grain size, D, we employ the spherical form factor proposed in the 1960s by Stein et al. to determine the size of spherulites in low-angle light scattering experiments.[29,30] We have compared numerical results obtained using the spherical form factor, quasi-Bragg analysis, and the correlation function approach and find that the trends developed below are the same in all cases. Analysis based on the spherical form factor results in grain sizes which are about 25% larger than the quasi-Bragg values, while the values obtained from the correlation function are smaller by about the same percentage.

Grain Size, *D*, and Lamellar Spacing, *d*. The spherical form factor

$$U = \left(\frac{4\pi}{\lambda}\sin\frac{\theta}{2}\right)R = qR \qquad (1)$$

exhibits a peak at a value $U = 4.0$.[29,30] For each scattering curve that exhibits a peak in the Ultra SAXS region, we can use this to obtain the grain size from the relation $D = 8/q_{max}$. We have tabulated grain sizes of the various annealed and unannealed specimens in Tables 1−3. The number of lamellar repeat distances contained in a typical grain is also shown as the ratio D/d. The remaining entries in Tables 1−3 will be discussed below. We also defer until later the method

Table 3. Values of Grain Size, *D*; Phase Fraction, ϕ; and Electron Density Differences, $(\Delta\rho)^2 = (\rho_{GB} - \rho_m)^2$ as a Function of Annealing Time at 75 °C for 9400/9000 Styrene−1,4-Butadiene (SB9)

annealing time	D (μm)	$(\Delta\rho)^2$	ϕ	D/d
none	0.58	8.75E−7[a]	0.098	20
5 min	0.66	2.20E−6	0.107	23
1 h	0.70	2.63E−6	0.103	24
2 h	1.08	7.40E−6	0.099	37
4 h[b]	2.09	9.13E−6	0.1[b]	72

[a] Read as 8.75×10^{-7}. [b] Peak falls outside range of Ultra SAXS machine. D is found with eq 5, assuming $\phi = 0.1$.

we used to obtain D for the few cases in which no resolvable peak was observed in the Ultra SAXS region of scattering.

The Contrast Factor and Grain Boundary Volume Fraction. There are features in the Ultra SAXS data that enable us to make certain internal consistency checks to support the proposed mechanism of scattering. In particular, the cartoon of Figure 6 indicates that $\Delta\rho^2$ should have an upper bound of $(\rho_s - \rho_m)^2$ or $(\rho_b - \rho_m)^2$, either of which to a good approximation for our polymers is equal to $[(\rho_s - \rho_b)/2]^2$. Extracting the contrast factor from our data would therefore provide one method to suport or discredit the proposed scattering mechanism. Also, Figure 6 suggests that the volume fraction of the grain boundary is small compared to the volume of material in the grain with mean density, ρ_m. If the analysis of the data indicates otherwise, the mechanism suggested in Figure 6 is in doubt. We use Porod's law and the scattering invariant, both of which are readily accessible characteristics of the scattering curves in the Ultra SAXS region, to test our mechanism. Porod's law constant, C_1, is obtained from the region to the right of the low-q scattering peak where intensities decrease with a q^{-4} dependence.

$$C_1 \equiv \frac{1}{2\pi}\lim_{q\to\infty} q^4 i = (S/V)(\rho_{GB} - \rho_m)^2 \qquad (2)$$

where i is the absolute desmeared intensity and S/V is the surface-to-volume ratio, which for the case of a sphere is equal to $6/D$. The invariant in this case is defined as the total area under the Iq^2 vs q plot associated with grain scattering and can be expressed as follows:

$$C_2 \equiv \frac{1}{2\pi^2}\int_0^\infty i(q)q^2\,dq = \phi(1-\phi)(\rho_{GB} - \rho_m)^2 \qquad (3)$$

where ϕ is the volume fraction of grain boundary material. Combining eqs 2 and 3 eliminates the contrast factor $(\Delta\rho)^2$ and yields

$$D = 6(V/S) = \frac{6C_2}{C_1\phi(1-\phi)} \qquad (4)$$

This equation can be solved for ϕ because the grain size D has been determined from the spherical form factor and the Ultra SAXS peak locations.

Values of ϕ are given in Tables 1−3. Over the range of grain sizes in the materials studied (spanning a factor of 4 from about 0.5 to 2 μm), the volume fraction of the grain boundary material remains essentially constant at $\phi = 0.1$. At $\phi = 0.1$ the grain size of 0.81 μm for polymer SB15 (14800/14100) corresponds to a grain boundary thickness of about 140 Å, which is less than

Table 4. Summary of Results of KR03 Resin Swelled with Various Amounts of Cumene

% polymer (ϕ_p)	d (Å)	D (μm)	ϕ_{GB}	$D_0 = D\phi_p^{1/3}$	D/d
1.00	318	1.35	0.104	1.35	42
0.66	343	1.56	0.102	1.36	45
0.57	389	1.59	0.095	1.32	41
0.44	440	1.85	0.1[a]	1.41	42
0.29	479	2.07	0.1[a]	1.37	43

[a] No peak in detectable range. D is found from eq 5, assuming $\phi = 0.1$.

one repeat distance of the block copolymer morphology, a result which is consistent with some TEM evidence.[19−23] A variation in ϕ from about 0.15 to about 0.05 over the range of grain sizes studied would result in a constant grain boundary thickness of 140 Å. Clearly more studies are needed, over a wider range of grain sizes, to elucidate these issues more definitively. At present we emphasize only the point that a value of ϕ around 0.1 is very consistent with the proposed model of Figure 6.

A second consistency check involves the magnitude of the contrast factor $(\Delta\rho)^2$ which appears in both eqs 2 and 3. Using the experimentally determined values of the Porod constant, C_1, and the surface-to-volume ratio from the spherical form factor ($S/V = 6/D$), we determined the values of $(\Delta\rho)^2$ which appear in Tables 1−3. For all three copolymers, this contrast factor tended to increase with annealing time at 75 °C. In all cases, the value is considerably less than the value of $(\rho_s - \rho_m)^2$ or $(\rho_b - \rho_m)^2$, which is 8.4×10^{-5} for the styrene−1,2-butadiene copolymer and approximately 4×10^{-4} for the styrene−1,4-butadiene copolymer. Once again, these results are entirely consistent with the mechanism suggested by Figure 6.

Estimating Grain Size in the Absence of the Low-*q* Peak. Figure 4 shows the scattering profiles for the 9400/9000 styrene−1,4-butadiene block copolymer (SM9) cast from chloroform. The peak associated with grains shifts to the left with increasing annealing time, and after annealing 4 h, the low-q peak is no longer resolvable. It is possible, however, to estimate D using eq 4. The data on the 4 h annealed sample provide reliable values of C_1 and C_2 in the absence of the low-q peak. The required value of ϕ cannot be determined independently, but over the range of samples examined here, ϕ is essentially constant at a value of 0.1. Thus, assuming $\phi = 0.1$ and using the experimentally determined values of C_1 and C_2, eq 4 provides the desired value of D. Table 3 indicates that the grain size estimated in this way is consistent with the trends of the overall set of results on sample SB9.

Swelling KR03 with a Nonvolatile Solvent. To dispel the belief that the scattering at very low values of q is dominated by the presence of voids, pellets of KR03 resin were swelled with various amounts of cumene. Absolute intensity vs q scattering profiles of the pure pellet and the four swollen samples are shown in Figure 5. The scattering profiles of the pellet and two of the swollen samples show low-q peaks and can be analyzed using the spherical form factor. The two samples with the most cumene do not show peaks and are analyzed under the assumption $\phi = 0.1$. Results are presented in Table 4. First we note that the lamellar repeat distance, d, increases as the block copolymer is swollen with increasing amounts of cumene. The grain size D also increases with cumene swelling, and since the ratio of D/d is nearly constant, it is apparent that both length scales are increasing in the same fashion. That both length scales, d and D, are proportional to the inverse cube root of polymer volume fraction is apparent from the essentially constant value of the product $D_0 = D\phi_p^{1/3}$, shown in the fifth column of Table 4.

Conclusions

Simultaneous determination of the morphological length scale, d, and the grain size D in a heterogeneous block copolymer is possible through the use of Ultra SAXS measurements. The d spacing was revealed directly in the data by the appearance of Bragg peaks in the relevant range of scattering angle. The block copolymer specimens also show peaks in the Ultra SAXS range. A value of grain size, D, can be found from these scattering profiles through the use of the spherical form factor. Use of the invariant and Porod's law validated the proposed mechanism via calculation of reasonable and consistent values of the electron density difference and the volume fraction of the grain boundary material. For scattering profiles that do not show a peak, use of the Porod region of the grain scattering mechanism and the invariant facilitated a reliable estimate of grain size D assuming the phase fraction of grain boundary, ϕ, is 0.1. Swelling KR03 resin with the low-volatility solvent cumene refutes the contention that the observed scattering at very low values of q is dominated by microscale voids.

Acknowledgment. We thank Gabrielle Long and Zugen Fu from the National Institute of Standards and Technology for their assistance in the use of the Ultra SAXS beamline at Brookhaven. Mike Frongillo of the CMSE (NSF/MRSEC) Electron Microscopy facility at MIT is acknowledged for his expertise and patience. The NSF MRSEC program is also acknowledged for partial support of the research. Professor Thomas Russell provided valuable insights in several helpful discussions with the authors.

References and Notes

(1) Keller, A.; Pedemonte, E.; Willmouth, F. M. *Nature* **1970**, *225*, 538.
(2) Garetz, B. A.; Balsara, N. P.; Dai, H. J.; Wang, Z.; Newstein, M. C. *Macromolecules* **1996**, *29*, 4675.
(3) Balsara, N. P.; Dai, H. J.; Watanabe, H.; Sato, T.; Osaki, K. *Macromolecules* **1996**, *29*, 3507.
(4) Balsara, N. P.; Dai, H. J.; Kesani, P. K.; Garetz, B. A.; Hammouda, B. *Macromolecules* **1994**, *27*, 7406.
(5) Garetz, B. A.; Newstein, M. C.; Dai, H. J.; Jonnalagadda, S. V.; Balsara, N. P. *Macromolecules* **1993**, *26*, 3151.
(6) Balsara, N. P.; Garetz, B. A.; Dai, H. J. *Macromolecules* **1992**, *25*, 6072.
(7) Csernica, J.; Baddour, R. F.; Cohen, R. E. *Macromolecules* **1987**, *20*, 2468.
(8) Csernica, J.; Baddour, R. F.; Cohen, R. E. *Macromolecules* **1989**, *22*, 1493.
(9) Myers, R. T.; Cohen, R. E.; Karbach, A., to be submitted to *Macromolecules*.
(10) Hashimoto, T.; Nagatoshi, K.; Todo, A.; Hasegawa, H.; Kawai, H. *Macromolecules* **1974**, *7*, 364.
(11) Hashimoto, T.; Shibayama, M.; Kawai, H. *Macromolecules* **1980**, *13*, 1237.
(12) Long, G. G.; Jemian, J. R.; Weertman, J. R.; Black, D. R.; Burdette, H. E.; Spal, R. *J. Appl. Crystallogr.* **1991**, *24*, 30.
(13) Fodor, L. M.; Kitchen, A. G.; Baird, C. C. *ACS Organ. Coat. Plast. Chem. Prepr.* **1974**, *34*, 130.
(14) Gebizlioglu, O. S.; Argon, A. S.; Cohen, R. E. *Polymer* **1985**, *26*, 519.
(15) Lake, J. A. *Acta Crystallogr.* **1967**, *23*, 191.

(16) Murthy, N. S.; Akkapeddi, M. K.; Otis, W. J. *Macromolecules* **1998**, *31*, 142.
(17) Murthy, N. S.; Zero, K. *Polymer* **1997**, *38*, 1021.
(18) Butler, M. F.; Donald, A. M. *Macromolecules* **1998**, *31*, 6234.
(19) Nishikawa, Y.; Kawada, H.; Hasegawa, H.; Hashimoto, T. *Acta Polym.* **1993**, *44*, 247.
(20) Gido, S. P.; Gunther, J.; Thomas, E. L.; Hoffman, D. *Macromolecules* **1993**, *26*, 4506.
(21) Gido, S. P.; Thomas, E. L. *Macromolecules* **1994**, *27*, 849.
(22) Gido, S. P.; Thomas, E. L. *Macromolecules* **1994**, *27*, 6137.
(23) Gido, S. P.; Thomas, E. L. *Macromolecules* **1997**, *30*, 3739.
(24) Mayes, A. M.; Kumar, S. K. Tailored Polymer Surfaces. *MRS Bull.* **1997**, *22* (1), 43−47.
(25) Pine, D. J.; Weitz, D. A.; Zhu, J. X.; Herboltzheimer, E. *J. Phys.* (*Paris*) **1990**, *51*, 2101.
(26) Durian, D. J.; Weitz, D. A.; Pine, D. J. *J Phys: Condens. Matter* **1990**, *2*, SA433.
(27) Zhu, J. X.; Pine, D. J.; Weitz, D. A. *Phys. Rev. A* **1991**, *44*, 3948.
(28) Glatter, O.; Kratky, O. *Small Angle X-Ray Scattering*; Academic Press: New York, 1982.
(29) Stein, R. S.; Rhodes, M. B. *J. Appl. Phys.* **1960**, *31*, 1873.
(30) Clark, R. J.; Miller R. L.; Stein, R. S. *J. Polym. Sci.* **1960**, *42*, 275.

MA9816618